Choice of Monomer Partition Model in Mathematical Modeling of Emulsion Copolymerization Systems

LUIS M. GUGLIOTTA, GURUTZE ARZAMENDI, and JOSÉ M. ASUA*

Grupo de Ingeniería Química, Departamento de Química Aplicada, Facultad de Ciencias Químicas, Universidad del País Vasco, Apdo. 1072, 20080 San Sebastián, Spain

SYNOPSIS

A criterion for the choice of the monomer partition model in mathematical modeling of emulsion copolymerization systems is presented. In order to develop this criterion, seeded emulsion copolymerizations of several monomer systems with a wide variety of reactivity ratios and water solubilities were simulated using monomer partition models of different complexity. The simulations included different processes, solids contents, and amounts of seed. The criterion for the choice of the monomer partition model was made on the basis of using the simplest but sufficiently accurate model. © 1995 John Wiley & Sons, Inc.

INTRODUCTION

In bulk and solution polymerizations, reactions occur in a single homogeneous phase. However, in emulsion polymerization, several phases can be present in the reactor: micelles, monomer droplets, polymer particles, and the dispersion medium. Consequently, the polymerization progress depends on the kinetic constants and on the concentration of the reactive species in the polymerization loci. In order to accurately describe emulsion polymerization systems by means of mathematical models, it is of paramount importance to implement a reliable prediction of monomer concentration in the different phases. The values of the concentrations and concentration ratios of monomers in the latex particles are key parameters in determining the polymerization rate, the copolymer composition, and the polymer structure. The monomer concentration in the polymer particles may also influence the rate of free-radical exit from latex particles, which in turn influences the rate of polymerization.

Under most circumstances, the rate of mass transfer of monomer between the different phases of the system is high enough for thermodynamic equilibrium of monomers between phases to be achieved.

For the estimation of the monomer concentration in the different phases under thermodynamic equilibrium conditions, the equilibrium equations have to be solved together with the material balances. While the material balances give rather general equations, several types of equilibrium equations can be used: Morton equations,[1-3] semiempirical equations based on simplifications of the Morton equations,[4-7] and equations based on constant partition coefficients.

For emulsion homopolymerization systems, Morton et al.[1] developed a model based on the classical Flory–Hüggins[8,9] lattice theory for monomer-polymer mixtures. The model includes an interfacial energy term and states that the increase in surface energy on swelling compensates for the free energy gain of mixing. Guillot[2] extended the thermodynamic monomer partitioning treatment of Morton to describe the monomer distribution during emulsion copolymerization by introducing interaction terms for the monomers. The equations are presented in Appendix I. This approach was used not only for the polymer particles, but also for the aqueous and monomer phases. However, Ugelstad[3] stressed the questionable use of the Flory–Hüggins model for evaluating the free energy of mixing for molecules that are neither chain like nor very different in size. In this case, the equations derived from the Flory–Hüggins theory are semiempirical relationships, and the parameters involved are transformed into adjustable coefficients. To over-

* To whom correspondence should be addressed.

Journal of Applied Polymer Science, Vol. 55, 1017–1039 (1995)
 CCC 0021-8995/95/071017-23

come this problem when monomers of limited solubility in water are utilized, Henry's law can be employed to model the droplets-aqueous phase equilibrium,[3] even in the presence of polymer particles.[4-7] In spite of these limitations, Morton's extension of the Flory–Hüggins theory for polymeric solutions has been widely used to estimate the concentrations of the monomers in emulsion copolymerization systems. References that were used in this study[10-20] are just a few examples of its application for the modeling and control of emulsion copolymerization systems.

The thermodynamic equations provide the most complete description of the swelling of polymer particles with monomers, but include a rather large number of parameters whose accurate estimation requires extensive work.

Maxwell, German, and coworkers[4-7] presented a semiempirical approach, valid for monomers of limited solubility in water, where the swelling of latex particles with monomers is calculated from the saturation swelling concentration of the homopolymers. This approach does not include any parameter, but experimental values of the saturation swelling volume fraction of the homopolymers are needed. This approach accounts for the following experimental evidence: during intervals I and II, the monomer ratio in the latex particles is equal to the monomer ratio in the droplets; the relationship between the concentration of monomer in the aqueous and the droplet phases obeys Henry's law for partially water soluble monomers, both in the absence and presence of monomer swollen latex particles; the overall concentration of monomer in the latex particles is approximately a linear function of the fraction of the monomers in the droplet phase; the partition coefficient between polymer particles and the aqueous phase does not remain constant, but decreases during interval III.[4,6,21-23]

Most of the computer time required to solve the mathematical models in emulsion polymerization systems is devoted to the calculation of the monomer partitioning. This becomes critical for on-line control in emulsion polymerization reactors.[24,25] The computational effort increases with the complexity of the equilibrium equations, namely, equations based on monomer partition coefficients are easier to solve than those of the Maxwell model, which are easier to solve than those based on the Flory–Hüggins theory. In addition, the number of unknown parameters, and hence the number of experiments required for their estimation, is much larger for the Morton model than for the other models. On the other hand, a rule of the thumb, well known among emulsion polymerization practitioners, is that the monomer concentration ratio in the polymer particles is, for practical uses, equal to that in the monomer droplets, and hence approximately equal to the average monomer concentration ratio in the reactor. This kind of practical knowledge seems to discourage the inclusion of complex monomer partitioning models in the mathematical modeling of emulsion polymerization systems. However, there is considerable experimental evidence that, for some systems, monomer partitioning affects the copolymer composition.[26-28]

Taking into account the considerable effort needed to estimate the parameters of the equilibrium equations and the large amount of computer time required for the calculation of the monomer partitioning, it would be interesting to have available a criterion of the level of complexity of the monomer partition equations that must be included in the mathematical model of a given emulsion polymerization system to achieve accurate model predictions.

In the present work, an attempt to develop such a criterion by mathematical simulation is made. Seeded emulsion copolymerizations of four monomer systems with a wide variety of reactivity ratios and water solubilities were considered: butyl acrylate (BuA)/styrene (St); vinyl acetate (VAc)/methyl acrylate (MA); VAc/BuA; and St/methacrylic acid (MAA). The effect of the complexity of the monomer partition equations, type of process, solids contents, and amount of seed on the time evolution of the conversion and copolymer composition was investigated.

SIMULATIONS

The copolymer systems studied were:

1. BuA/St: Sparingly water soluble monomers (BuA = 0.14 g/100 g of water; St = 0.06 g/100 g of water), with different reactivity ratios ($r_{BuA} = 0.2$; $r_{St} = 0.75$).
2. VAc/MA: Rather water soluble monomers (VAc = 2.5 g/100 g of water; MA = 5 g/100 g of water), the more water soluble being the more reactive ($r_{VAc} = 0.1$; $r_{MA} = 9$).
3. VAc/BuA: Monomers of different water solubilities (VAc = 2.5 g/100 g of water; BuA = 0.14 g/100 g of water), the more soluble in water being the less reactive ($r_{VAc} = 0.037$; $r_{BuA} = 6.35$).
4. St/MAA: One sparingly water soluble monomer (St = 0.06 g/100 g of water) and one

completely water soluble monomer (MAA) with different reactivity ratios (r_{St} = 0.25; r_{MAA} = 0.55).

The following seeded emulsion copolymerization processes were considered:

1. batch emulsion polymerization;
2. semicontinuous "starved" emulsion polymerization. In this context, starved means that both monomers were fed slowly into the reactor and, after some monomer accumulation in the reactor, an equilibrium between monomer feed rate and polymerization rate was achieved;
3. semicontinuous optimal "semistarved" emulsion polymerization. In this process the reactor is initially charged with all the less reactive monomer plus the amount of the more reactive monomer needed to initially form a copolymer with the desired composition; the remaining monomer is added at a flow rate that ensures the formation of a copolymer of constant composition.[13,17,29,30]

Solids content should have a significant effect on the monomer partitioning, therefore different solids contents were considered in the simulations:

1. low solids contents (10 wt %), often used in basic kinetic studies;[31]
2. medium solids content (30 wt %). Most of the fundamental studies reported in the open literature are in this range;[10–20]
3. high solids content (55 wt %), representative of the solids content used in industrial practice.

Furthermore, the influence of the amount of seed was analyzed. The initial seed/total monomer ratio was modified between 0.03 and 0.15 (the smallest amount of seed polymer was included in an attempt to simulate a case close to unseeded emulsion polymerizations but avoiding the use of a nucleation model).

The models used to calculate the monomer partition are given in Appendix I and include: the Morton extension of the Flory–Hüggins theory,[3] the semiempirical approximation by Maxwell et al.,[4–7] and the constant monomer partition coefficients.

For the resolution of the set of nonlinear algebraic equations given in Appendix I, the algorithm proposed by Armitage et al.[32] was used when the Morton model was considered; the algorithm developed in Appendix II was employed when the Maxwell semiempirical equations were considered; and a technique inspired by the work of Omi[33] was utilized for the case of constant partition coefficients. For the case of constant partition coefficients, the main improvement of the algorithm used in the present article is that the set of equations to be solved does not depend on the presence of monomer droplets in the system. Therefore, the presence of monomer droplets does not have to be systematically checked during the integration of the mathematical model and this leads to substantial computer time savings. The mathematical structure of the Maxwell model makes it necessary to check the presence of monomer droplets in the system prior to solving the monomer partition equations. This increases the computer time required. The algorithm developed by Armitage et al.[32] for the case in which the equilibrium is described in terms of the Morton model allows the calculation of the monomer partitioning without checking the existence of monomer droplets in the system. Predictions of conversion and copolymer composition evolutions were made through mathematical models previously described.[13,19]

The Morton model provides the most complete description of the monomer partitioning; therefore it was assumed that the predictions calculated using this model represented the actual behavior of the emulsion polymerization system. The predictions obtained using the simpler models (Maxwell approach and constant partition coefficients) were regarded as approximations whose usefulness was given by the difference with the predictions of the Morton model.

Most of the parameters involved in the Morton model were taken from the literature. The saturation swelling volume fractions included in the Maxwell equations were obtained from literature values.[34] The constant monomer partition coefficients were calculated from saturation data of the monomers in water and in the polymer particles.[34,35]

Batch Emulsion Polymerization

BuA/St Copolymerization

Figure 1 presents the comparison between the predictions of the three models using the parameters and reaction conditions given in Table I for a recipe with a 30 wt % solids content, a seed/total monomer volumetric ratio of 0.1, and a BuA/St molar ratio equal to one. The predictions include the evolution of the instantaneous conversion of monomers A and B (x_A, x_B), the overall conversion (x); and the cu-

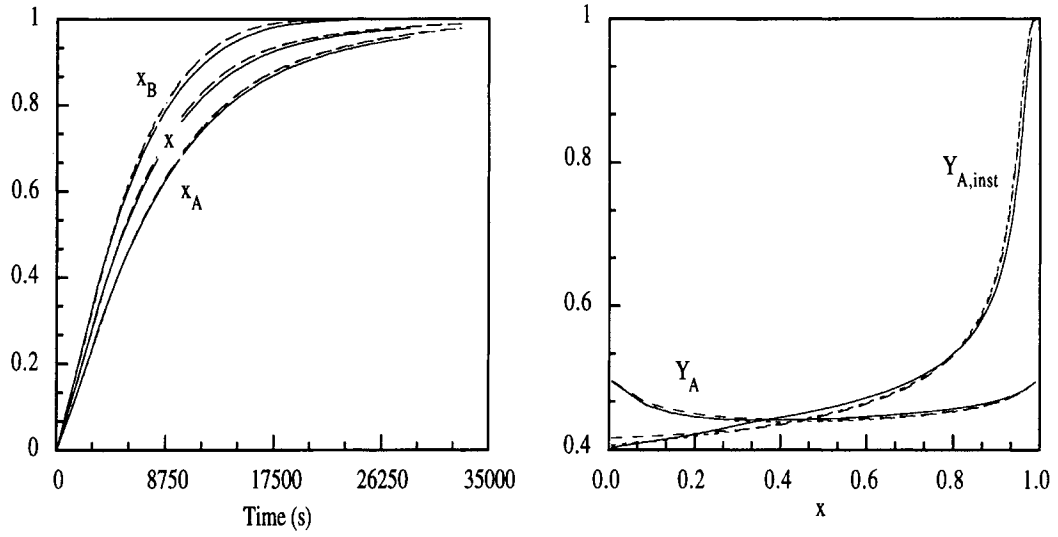

Figure 1 Time evolution of the conversions and copolymer compositions calculated with the three partition models for the batch emulsion copolymerization of BuA/St with a 30 wt % solids content and a seed/monomer ratio of 0.1. (—) Morton, (· · ·) Maxwell, and (- - -) constant partition coefficients.

mulative (Y_A) and instantaneous molar copolymer compositions ($Y_{A,inst}$) referred to BuA. It can be seen that the changes in the evolution of both the conversions and the copolymer compositions due to the monomer partition model fell within the experimental error.

Figure 2 presents the effect of the solids content on the predictions of the three models. It can be seen that when the solids content increased, the time evolutions of conversions and copolymer compositions became independent of the partition model. On the other hand, for a 10% solids content, the predictions of the Maxwell model were close to those of the model using constant partition coefficients, but significantly different from the ones obtained with the Morton model.

Table I Parameters and Reaction Conditions Used in Simulations of Emulsion Copolymerizations of BuA (A) and St (B)

k_{pAA}, k_{pBB}, k_{pAB}, k_{pBA} (cm^3/mol s)[36]	2.47×10^5	4.82×10^5	1.23×10^6	6.43×10^5
k_{tAA}, k_{tBB}, k_{tAB}, k_{tBA}(cm^3/mol s)[36]	5.61×10^8	2.10×10^{12}	3.43×10^{10}	3.43×10^{10}
k_{fAA}, k_{fBB}, k_{fAB}, k_{fBA} (cm^3/mol s)[36]	34.00	19.46	25.73	25.73
k_I (s^{-1})[36]	0.5×10^{-5}			
χ_{AW}, χ_{BW}, χ_{AB}, χ_{BA}[5]	4.2	3.6	0.26	0.42
χ_{WA}, χ_{WB}[3]	3.2	3.27		
$(1 - m_{AW})$[11], $(1 - m_{BW})$, $(1 - m_{AB})$, $(1 - m_{BA})$	−0.31	−0.11	−0.25	0.20
$(1 - m_{AP})$, $(1 - m_{BP})$, $(1 - m_{WA})$, $(1 - m_{WB})$[18]	1	1	0.24	0.10
χ_{APA}, χ_{BPB}, χ_{APB}, χ_{BPA}[37]	0.35	0.38	0.31	0.42
D_W, D_P (cm^2/s)[13]	10^{-5}	10^{-7}		
F, f[36]	6×10^{-3}	0.4		
σ (dyne/cm)[11]	4			
k_A^d, k_A^p, k_B^d, k_B^p[34,38]	740	480	1810	1080
$\phi^w_{A,sat}$, $\phi^W_{B,sat}$[38]	1.13×10^{-3}	5.52×10^{-4}		
$\phi^p_{A,sat}$, $\phi^p_{B,sat}$[34]	0.65	0.60		
A^0 (moles)	0.975			
I^0 (moles)	1.47×10^{-3}			
d_p^0 (nm)	70			
N_p	1.4×10^{17}			
W (cm^3)	570			

Note: The superscript numbers following the entries in the first column are reference numbers.

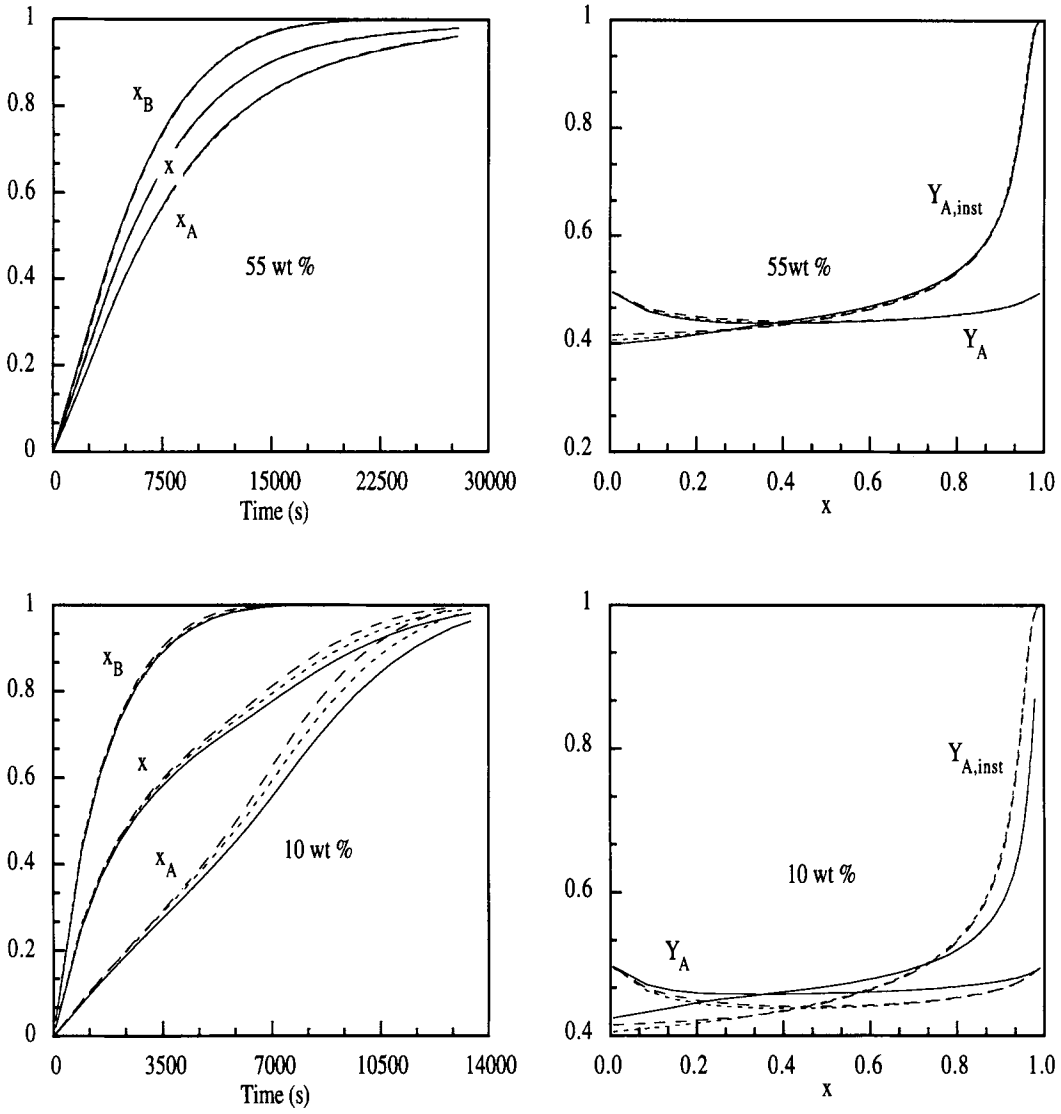

Figure 2 Effect of solids content on the predictions of the three monomer partition models for the batch emulsion copolymerization of BuA/St. (—) Morton, (· · ·) Maxwell, and (- - -) constant partition coefficients.

The effect of the seed/monomer ratio is presented in Figure 3, for a 30 wt % solids content. It can be seen that when the seed/monomer ratio was significantly decreased, that is the polymerization conditions approached those of unseeded processes, the predictions of the Morton model differed from those of the other two models, which were close to each other.

The simulations showed that for the batch seeded emulsion copolymerization of BuA and St, the predictions are independent of the monomer partition model for high solids content systems (55 wt %). For medium solids content systems (30 wt %) the predictions were independent of the monomer partitioning model when significant amounts of seed polymer were used (> 10%), but the predictions of the Morton model differed from those of the other two models when a small amount of seed was used. These differences were more acute for low solids content systems. In addition, the model based on constant partition coefficients gave almost the same predictions as those of the Maxwell model.

VAc/MA Copolymerization

Figure 4 presents the comparison between the predictions of the three models using the parameters and reaction conditions given in Table II for a 30 wt % solids content, a seed/total monomer volu-

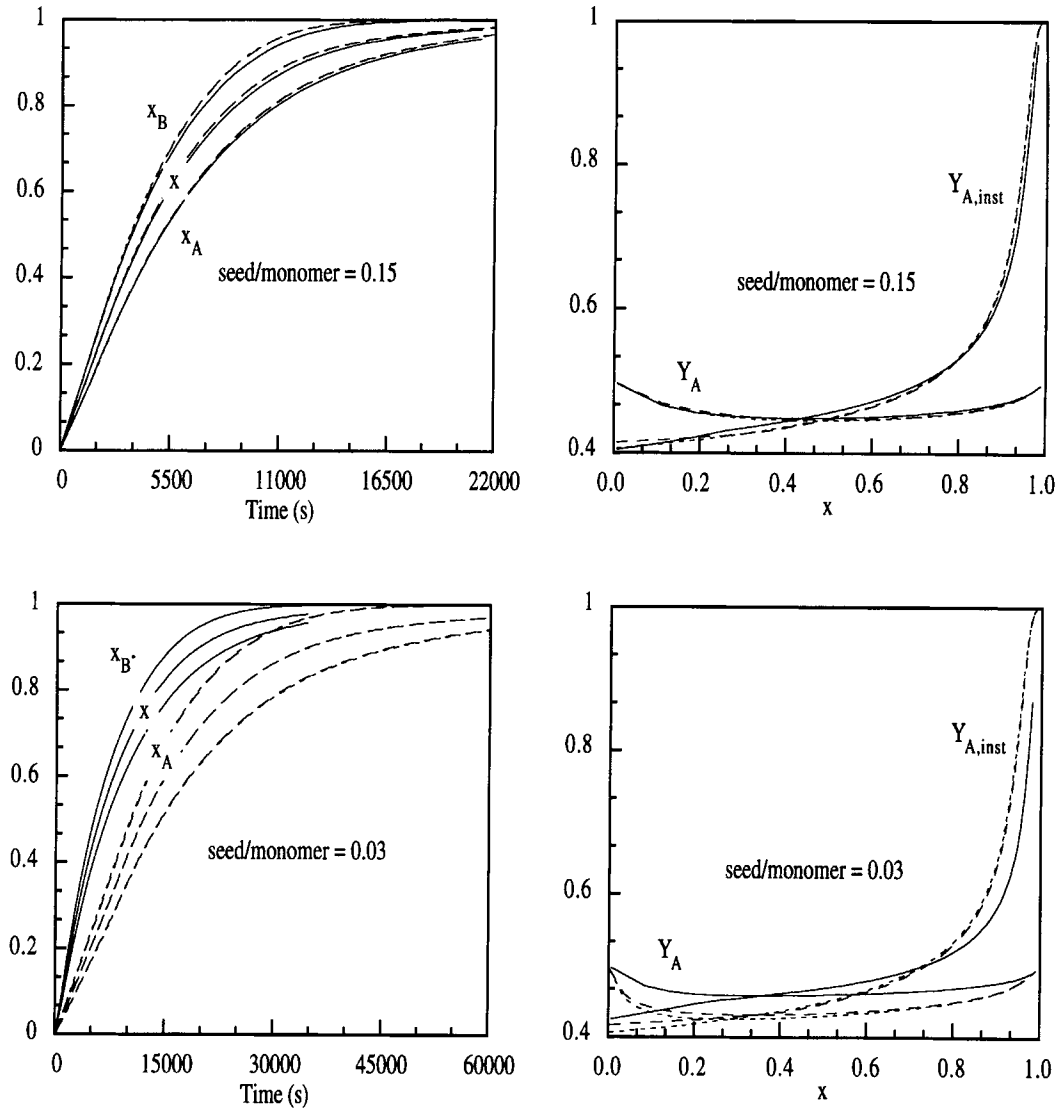

Figure 3 Effect of the seed/monomer ratio on conversion and copolymer composition profiles predicted by the models of (—) Morton, (• • •) Maxwell, and (- - -) constant partition coefficients in the batch emulsion copolymerization of BuA/St (30 wt % solids content).

metric ratio of 0.085, and a molar monomer ratio equal to one. It can be seen that the curves of x_A, x_B, x, Y_A, and $Y_{A,inst}$ obtained with the three different monomer partition models were practically identical.

The effect of solids content on the predictions of the three models is presented in Figure 5. It can be seen that for high solids content, both the conversions and copolymer compositions were independent of the monomer partition model. For low solids content, the conversion curves depend slightly on the partition model, but the composition vs. conversion profiles were independent of the partition model at all solids contents.

The effect of the seed/monomer ratio is presented in Figure 6 for a 30 wt % solids content. It can be seen that for the high seed/monomer ratio, the predicted copolymer composition and conversion profiles were independent of the monomer partition model. On the other hand, for the low seed/monomer ratio the predictions of the Morton model differed from those of the other two models. In addition, the predictions obtained by means of the constant partition and Maxwell models were very similar.

VAc/BuA Copolymerization

Figure 7 shows the results obtained with the three monomer partition models using the parameters and reaction conditions given in Table III for a 30 wt % solids content, a seed/total monomers volumetric

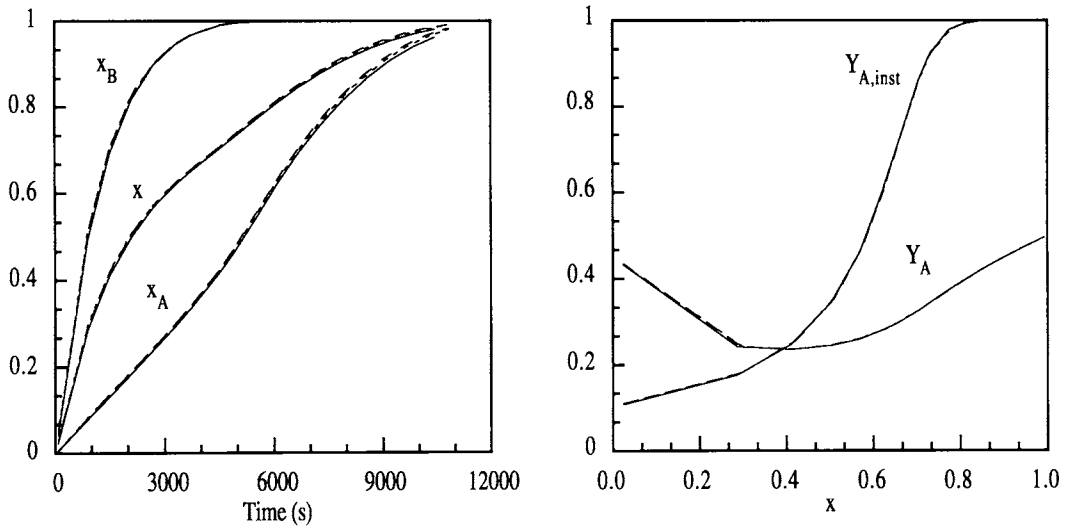

Figure 4 Time evolution of the conversions and copolymer compositions calculated with the three partition models for the batch emulsion copolymerization of VAc/MA with a 30 wt % solids content and a seed/monomer ratio of 0.085. (—) Morton, (· · ·) Maxwell, and (- - -) constant partition coefficients.

ratio of 0.05, and a molar monomer ratio equal to one. It can be seen that the monomer partitioning model had only a limited effect on both the conversion and copolymer composition profiles.

Figure 8 presents the effect of the solids content on the conversions and copolymer composition. It can be seen that the higher the solids content the more similar were the predictions of the copolymer composition of the Morton model and those of the other two models. Simulations carried out varying

Table II Parameters and Reaction Conditions Utilized in Emulsion Copolymerizations of VAc (A) and MA (B)

k_{pAA}, k_{pBB}, k_{pAB}, k_{pBA} (cm^3/mol s)[13]	0.23×10^7	0.21×10^7	0.23×10^8	0.23×10^6
k_{tAA}, k_{tBB}, k_{tAB}, k_{tBA} (cm^3/mol s)[13]	0.29×10^{11}	0.95×10^{10}	0.19×10^{11}	0.19×10^{11}
k_{fAA}, k_{fBB}, k_{fAB}, k_{fBA} (cm^3/mol s)[13]	0.40×10^3	0.20×10^2	0.60×10^2	0.20×10^2
k_I (s^{-1})[13]	0.58×10^{-5}			
χ_{AW}, χ_{BW}, χ_{AB}, χ_{BA}[13]	3.20	2.97	−0.139	−0.126
χ_{WA}, χ_{WB}[13]	8.65	4.37		
$(1 - m_{AW})$, $(1 - m_{BW})$, $(1 - m_{AB})$, $(1 - m_{BA})$[13]	0.63	0.32	−0.098	0.090
$(1 - m_{AP})$, $(1 - m_{BP})$, $(1 - m_{WA})$, $(1 - m_{WB})$[13]	1	1	−1.703	−0.471
χ_{APA}, χ_{BPB}, χ_{APB}, χ_{BPA}[13]	0.38	0.507	0.706	0.398
D_W, D_P (cm^2/s)[13]	10^{-7}	10^{-5}		
F, f[13]	0.006	0.6		
σ (dyne/cm)[13]	4			
k_A^d, k_A^p, k_B^d, k_B^p[34,35]	37	31	17	14
$\phi_{A,sat}^w$, $\phi_{B,sat}^w$[35]	0.0268	0.0589		
$\phi_{A,sat}^p$, $\phi_{B,sat}^p$[34]	0.85	0.85		
A^0 (moles)	0.416			
I^0 (moles)	0.314×10^{-3}			
d_p^0 (nm)	50			
N_p	1×10^{17}			
W (cm^3)	185			

Note: The superscript numbers following the entries in the first column are reference numbers.

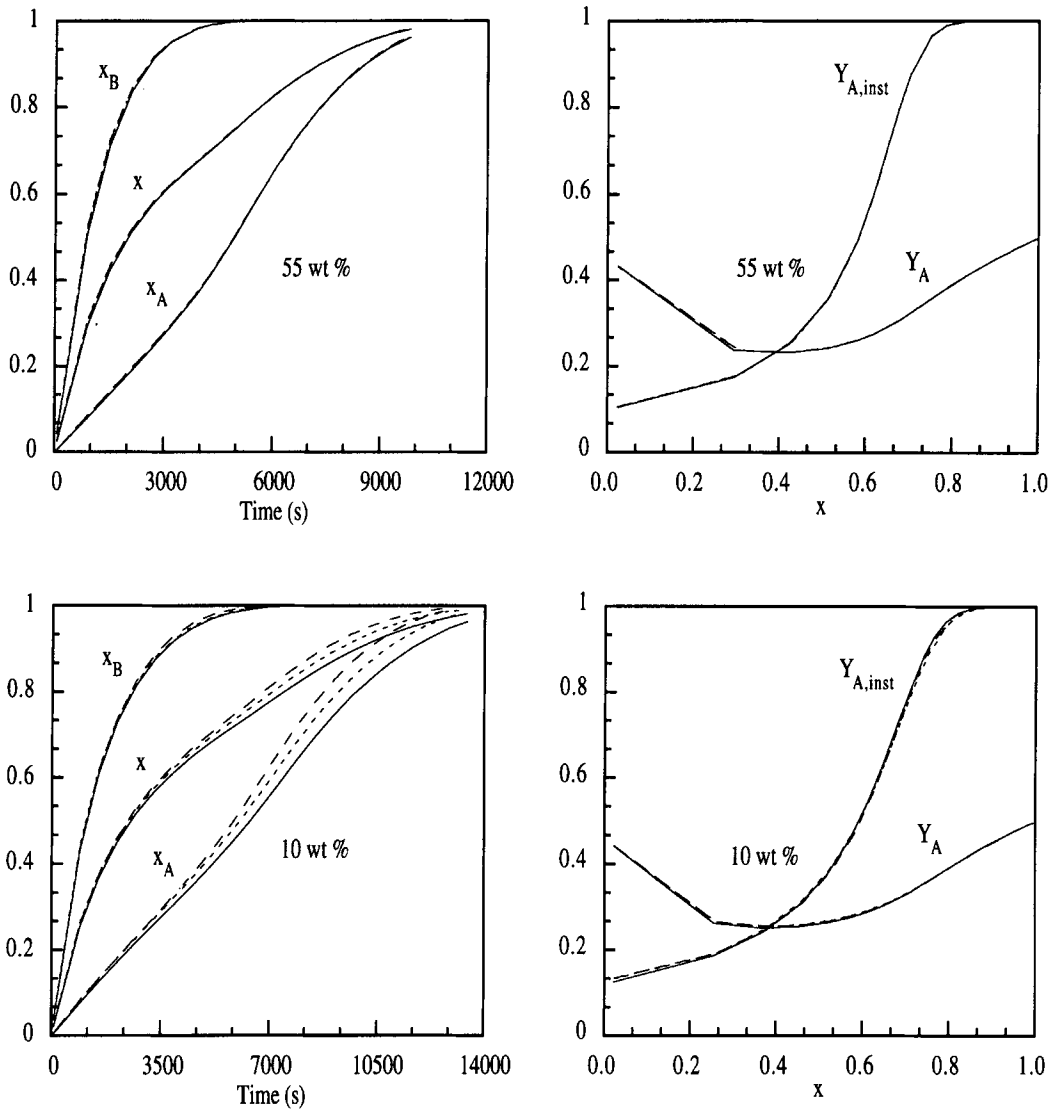

Figure 5 Effect of solids content on the predictions of the three monomer partition models for the batch emulsion copolymerization of VAc/MA. (—) Morton, (· · ·) Maxwell, and (- - -) constant partition coefficients.

the amount of seed showed that the predictions of the three models for solids contents greater than 30 wt % agreed reasonably well for seed/monomer ratios in the range of 0.03–0.15.

St/MAA Copolymerization

Table IV shows the reaction conditions and parameter values used in the simulations of batch seeded emulsion copolymerization of St and MMA. The recipe included a solids content of 30 wt %, a seed/total monomer volumetric ratio of 0.05, and a monomer molar ratio (St/MAA) equal to 3.3. Figure 9 presents a comparison of the copolymer compositions predicted by the Morton model and those obtained with constant partition coefficients. The Maxwell model was not used because it is only valid for monomers of limited solubility in water, and MAA is completely soluble in water. It can be seen that the predictions differed significantly. This difference decreased slightly when the solids content and the seed/monomer ratio increased to 55 and 0.15 wt %, respectively, but even in this case the discrepancies were large enough to discourage the use of constant partition coefficients.

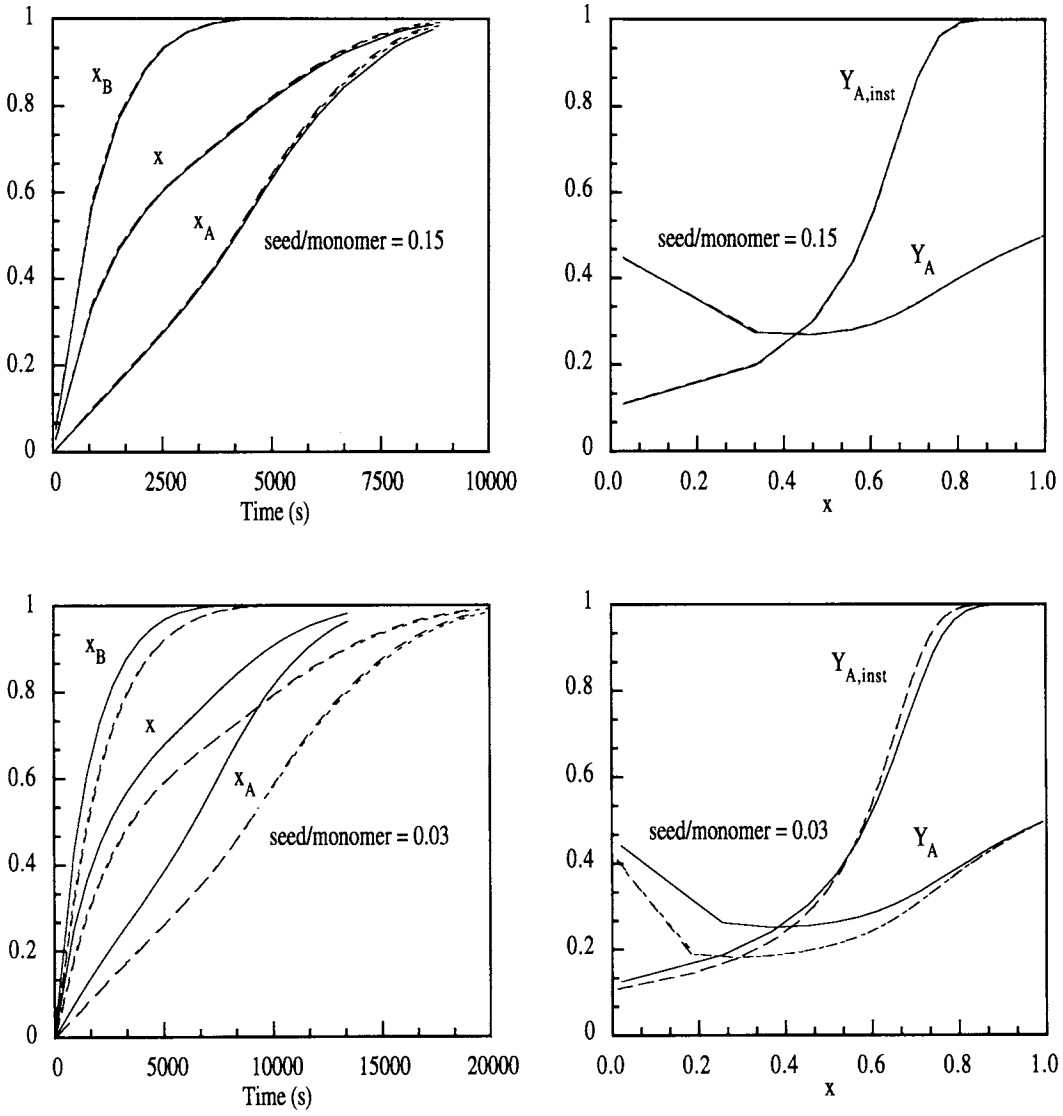

Figure 6 Effect of the seed/monomer ratio on conversion and copolymer composition profiles predicted by the models of (—) Morton, (· · ·) Maxwell, and (---) constant partition coefficients in the batch emulsion copolymerization of VAc/MA with a 30 wt % solids content.

Semicontinuous Emulsion Polymerization Under Starved Conditions

BuA/St Copolymerization

Figure 10 presents the evolution of the instantaneous conversion and the instantaneous copolymer composition calculated with the three monomer partition models using the parameters and reaction conditions in Table I, and a total volumetric feed rate of 0.5×10^{-2} cm^3/s for different solids contents. It can be seen that the evolution of the conversion predicted by the Morton model was different from those predicted by the other two models, which were similar. The difference between the Morton model and the other models was within the experimental error for high solids contents (55 wt %) but significant at low solids contents (10 wt %). In addition the greater the amount of initial seed, the lower the difference between the predictions of the different models.

VAc/MA Copolymerization

Figure 11 shows the effect of both the solids content and monomer partition model on the simulated results of the instantaneous conversion and instan-

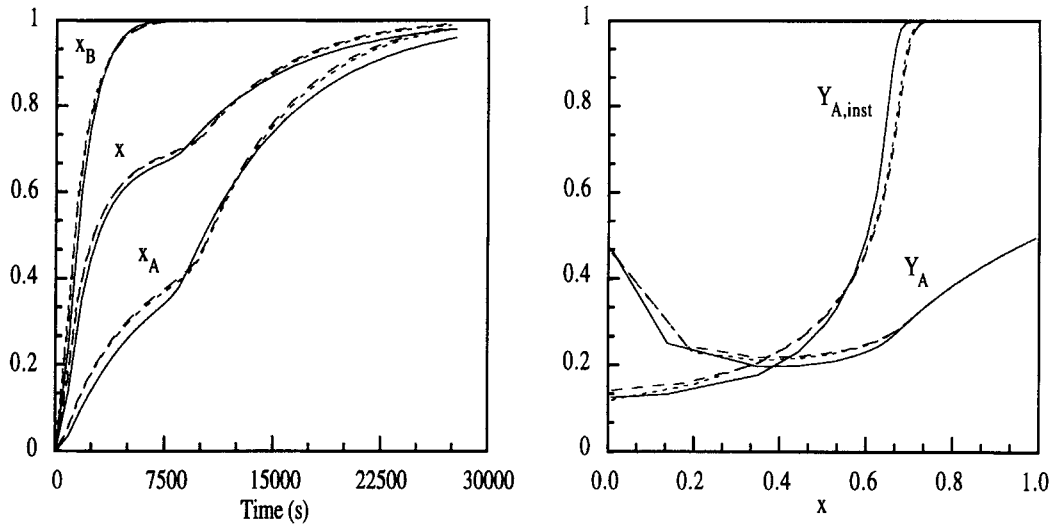

Figure 7 Time evolution of the conversions and copolymer compositions calculated with the three monomer partition models for the batch emulsion copolymerization of VAc/BuA with a 30 wt % solids content and a seed/monomer ratio of 0.05. (—) Morton, (· · ·) Maxwell, and (- - -) constant partition coefficients.

taneous copolymer composition obtained under starved conditions, using the parameters and operating conditions given in Table II, and a total volumetric feed rate of 0.3×10^{-2} cm^3/s. It can be seen that the predictions of the three models were close for 55 wt % solids content, whereas substantial differences were found for 10 wt % solids content. In addition, Figure 11 shows that, in contrast with the results obtained for the batch process, the predictions of the Maxwell model were better than those of the partition coefficients model. This difference was due to the fact that, in agreement with the ex-

Table III Parameters and Reaction Conditions Used in Simulations of Emulsion Copolymerizations of VAc (A) and BuA (B)

k_{pAA}, k_{pBB}, k_{pAB}, k_{pBA} (cm^3/mol s)[11]	0.23×10^7	0.126×10^6	0.635×10^8	0.198×10^5
k_{tAA}, k_{tBB}, k_{tAB}, k_{tBA} (cm^3/mol s)[11]	0.29×10^{11}	0.625×10^6	0.135×10^9	0.135×10^9
k_{fAA}, k_{fBB}, k_{fAB}, k_{fBA} (cm^3/mol s)[11]	0.4×10^3	0.34×10^2	0.34×10^2	0.4×10^3
k_I (s^{-1})[11]	0.613×10^{-5}			
χ_{AW}, χ_{BW}, χ_{AB}, χ_{BA}[11]	2.1	4.2	0.15	0.45
χ_{WA}, χ_{WB}[11]	5.6	3.2		
$(1 - m_{AW})$, $(1 - m_{BW})$, $(1 - m_{AB})$, $(1 - m_{BA})$[11]	0.63	−0.31	0.67	−2.03
$(1 - m_{AP})$, $(1 - m_{BP})$, $(1 - m_{WA})$, $(1 - m_{WB})$[11]	1	1	−1.703	0.237
χ_{APA}, χ_{BPB}, χ_{APB}, χ_{BPA}[11]	0.37	0.35	0.36	0.46
D_W, D_P (cm^2/s)[11]	1×10^{-7}	1×10^{-5}		
F, f[11]	0.006	0.5		
σ (dyne/cm)[11]	4			
k_A^d, k_A^p, k_B^d, k_B^p[11,34]	37	31	740	480
$\phi^w_{A,sat}$, $\phi^w_{B,sat}$[11]	0.0268	0.001352		
$\phi^p_{A,sat}$, $\phi^p_{B,sat}$[34]	0.85	0.65		
A^0 (moles)	0.654			
I^0 (moles)	0.907×10^{-3}			
d_p^0 (nm)	92.4			
N_p	1.9×10^{16}			
W (cm^3)	348			

Note: The superscript numbers following the entries in the first column are reference numbers.

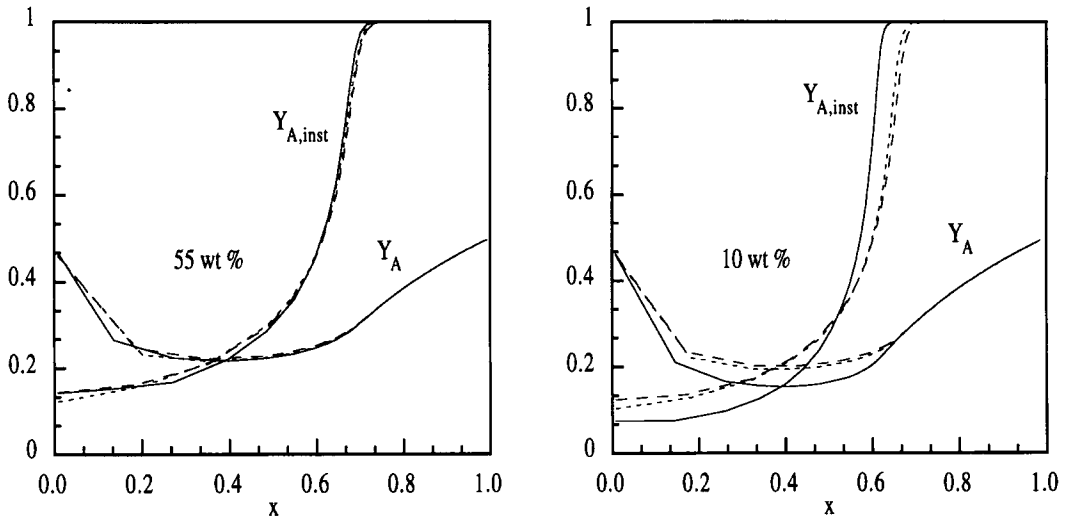

Figure 8 Effect of solids content on the predictions of the three monomer partition models in the batch emulsion copolymerization of VAc/BuA. (—) Morton, (· · ·) Maxwell, and (- - -) constant partition coefficients.

perimental results[4,6,21-23] and the estimations of the Morton model, the Maxwell model predicts that the monomer partition coefficients between the polymer particles and aqueous phase decrease when the polymer volume fraction in the polymer particles increases in the absence of monomer droplets, whereas they remain unchanged in the monomer partition coefficients model. Therefore, when the latter model is used under starved conditions (high polymer volume fractions in the polymer particles), the concentration of the monomers in the polymer particles is overestimated and hence the polymerization rate is higher and the copolymer more homogeneous than for the other two models.

VAc/BuA Copolymerization

Figure 12 presents the effect of both solids content and monomer partition model on the instantaneous conversion and instantaneous copolymer composi-

Table IV Parameters and Reaction Conditions Utilized in Simulations of Emulsion Copolymerizations of St (A) aand MAA (B)

k_{pAA}, k_{pBB}, k_{pAB}, k_{pBA} (cm^3/mol s)[15]	9.0×10^5	1.59×10^7	3.6×10^6	2.89×10^7
k_{tAA}, k_{tBB}, k_{tAB}, k_{tBA} (cm^3/mol s)[15]	2.5×10^{11}	1×10^{10}	5×10^{10}	5×10^{10}
k_{fAA}, k_{fBB}, k_{fAB}, k_{fBA} (cm^3/mol s)[15]	67.5	397.5	39.75	6.75
k_I (s^{-1})[15]	1.147×10^{-4}			
χ_{AW}, χ_{BW}, χ_{AB}, χ_{BA}[15]	8.07	7.85	2.98	2.20
χ_{WA}, χ_{WB}[15]	7.27	1.67		
$(1 - m_{AW})$, $(1 - m_{BW})$, $(1 - m_{AB})$, $(1 - m_{BA})$[15]	−0.11	−3.707	−0.357	0.263
$(1 - m_{AP})$, $(1 - m_{BP})$, $(1 - m_{WA})$, $(1 - m_{WB})$[15]	1	1	0.099	0.787
χ_{AP}, χ_{BP}[15]	0.35	3		
D_W, D_P (cm^2/s)[15]	10^{-7}	10^{-5}		
F, f[15]	0.006	0.6		
σ (dyne/cm)[15]	4			
k_A^d, k_A^p,[34,38] k_B^d, k_B^p[a]	1800	1200	6	3.6
A^0 (moles)	1.535			
I^0 (moles)	0.135×10^{-2}			
d_p^0 (nm)	28			
N_p	1×10^{18}			
W (cm^3)	494			

Note: The superscript numbers following the entries in the first column are reference numbers.
[a] Average estimated values.[15]

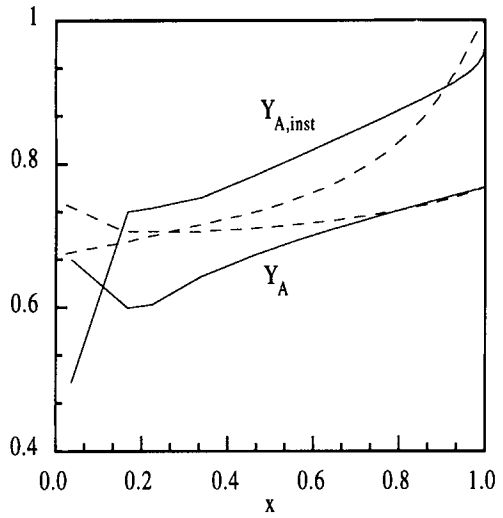

Figure 9 Comparison between the copolymer composition evolution predicted by the Morton model and that calculated using constant monomer partition coefficients for the batch emulsion copolymerization of St/MAA. (—) Morton and (---) constant partition coefficients.

tion calculated using the parameters and reaction conditions given in Table III, and a total feed rate of 0.1×10^{-3}, for the semicontinuous emulsion copolymerization of VAc and BuA, under starved conditions. It can be seen that the predictions of the three models were close to each other for a 55 wt % solids content, whereas substantial differences were found for 10 wt % solids content. In addition, the predictions of the Maxwell model were better than those of the partition coefficients model.

St/MAA Copolymerization

Figure 13 presents the effect of both solids content and the monomer partition model on the simulated results of the instantaneous conversion and instantaneous copolymer composition obtained under starved conditions for the semicontinuous emulsion copolymerization of St and MMA. The reaction conditions and the values of the parameters given in Table IV, a total volumetric feed rate of 0.5×10^{-1} cm^3/s and a molar ratio equal to 3.3, were used in the calculations. The Maxwell model was not used because it cannot be applied to completely water soluble monomers. Figure 13 shows that the predictions obtained using constant partition coefficients agreed quite well with those of the Morton model at high solids content, but that significant differences between the predictions of these models were found for low solids contents.

The greater the amount of seed, the lower the differences between the estimations of the different partition models. In addition, the more starved the process, the smaller the differences between the models. This means that the differences are reduced by increasing initiator and emulsifier concentrations and by decreasing the monomer feed rate.

Semicontinuous Optimal Semistarved Emulsion Polymerization

This process refers to a minimum-time optimal policy for copolymer composition control.[13,17,29,30] In order to apply this policy, the monomer feed rates have to be calculated in advance. In the present work, the approach proposed by Arzamendi et al.[13,17,29,30] was used. This approach is not described here and the reader is referred to other studies[13,17,29,30] for the details of the calculations. Because there is no interest in using this approach for low solids contents, simulations were carried out only for medium and high solids contents.

As explained previously, the Morton model was assumed to represent the actual behavior of the emulsion polymerization system. The comparison between this model and the simplified ones, namely the Maxwell and constant monomer partition coefficients models, was carried out as follows. First, the monomer feed rates were calculated by means of the approach of Arzamendi et al.[13,17,29,30] and using the three monomer partitioning models. Then, polymerizations using these monomer feed rates were simulated for the actual emulsion polymerization system, that is for that described by the Morton model. The monomer feed rates calculated by the Morton model will give the desired copolymer composition, but deviations from the desired value are expected to occur when the monomer feed rates calculated by means of the simplified monomer partitioning models are used. These deviations will provide a measure of the suitability of the simplified models.

BuA/St Copolymerization

Figure 14 presents the St feed rate profiles obtained with the different partition models, and the time evolution of the instantaneous copolymer composition referred to BuA calculated as described above for the recipe given in Table I. It can be seen that, due to the differences observed in the feed rate profiles and initial charges of St, the instantaneous copolymer compositions obtained using the monomer

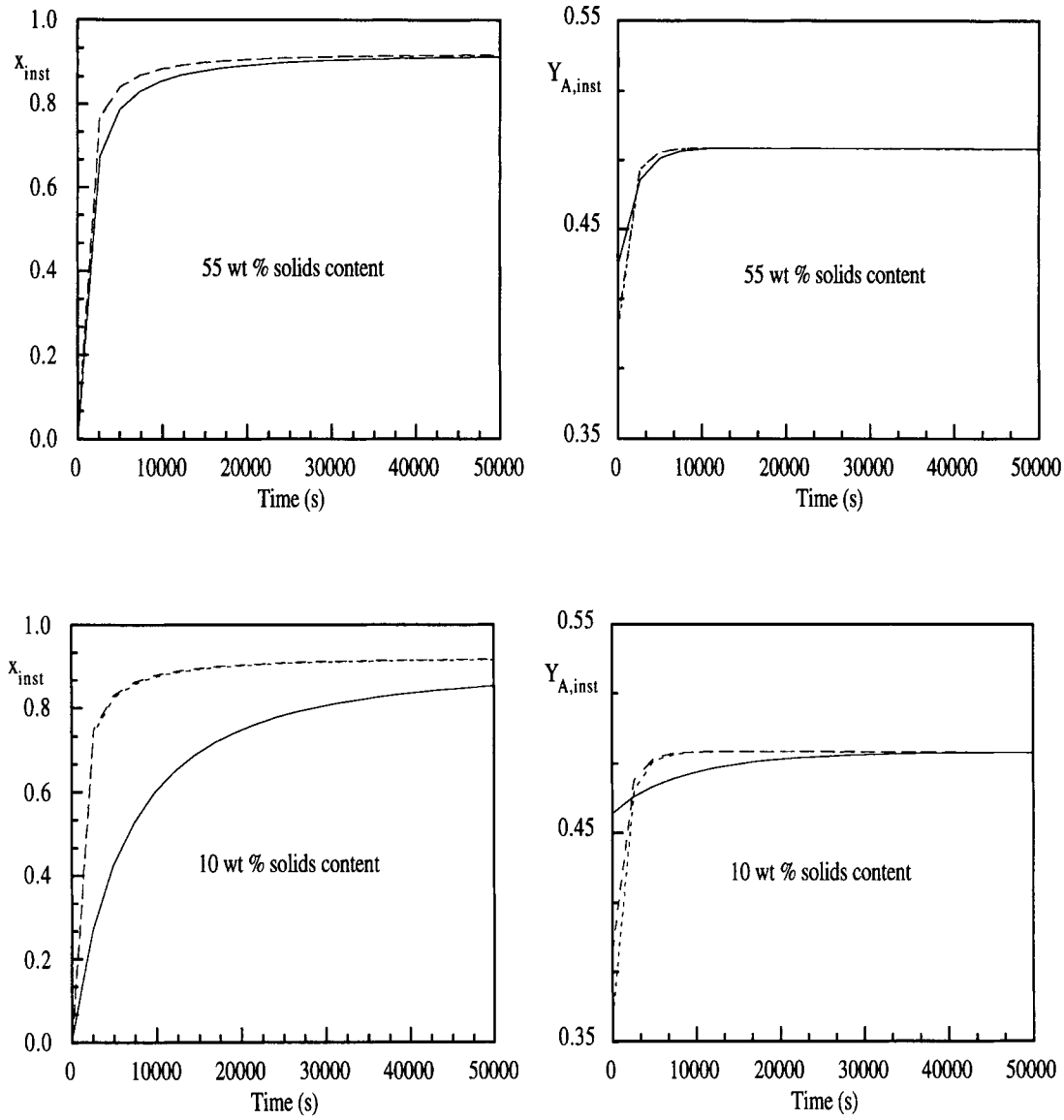

Figure 10 Effect of solids content on the evolution of the instantaneous conversion and the instantaneous copolymer composition calculated using the three monomer partition models for the semicontinuous emulsion copolymerization of St/BuA under starved conditions. (—) Morton, (· · ·) Maxwell, and (- - -) constant partition coefficients.

feed rates calculated with the Maxwell model and the constant monomer partition coefficients model deviated from the desired value. Nevertheless, the influence of the monomer partition model on the cumulative copolymer composition is much less and close to the experimental errors associated with the determination of the cumulative copolymer composition by a standard technique such as NMR. The effect of the monomer partition model decreased when solids content increased.

VAc/MA Copolymerization

Figure 15 presents the MA feed rate profiles obtained with the three partition models, and the time evolution of the instantaneous copolymer composition referred to VAc for a 30 wt % solids content recipe (Table II). It can be seen that the monomer partition model had a limited effect on the instantaneous copolymer composition. This effect is even lower for the cumulative copolymer composition and for

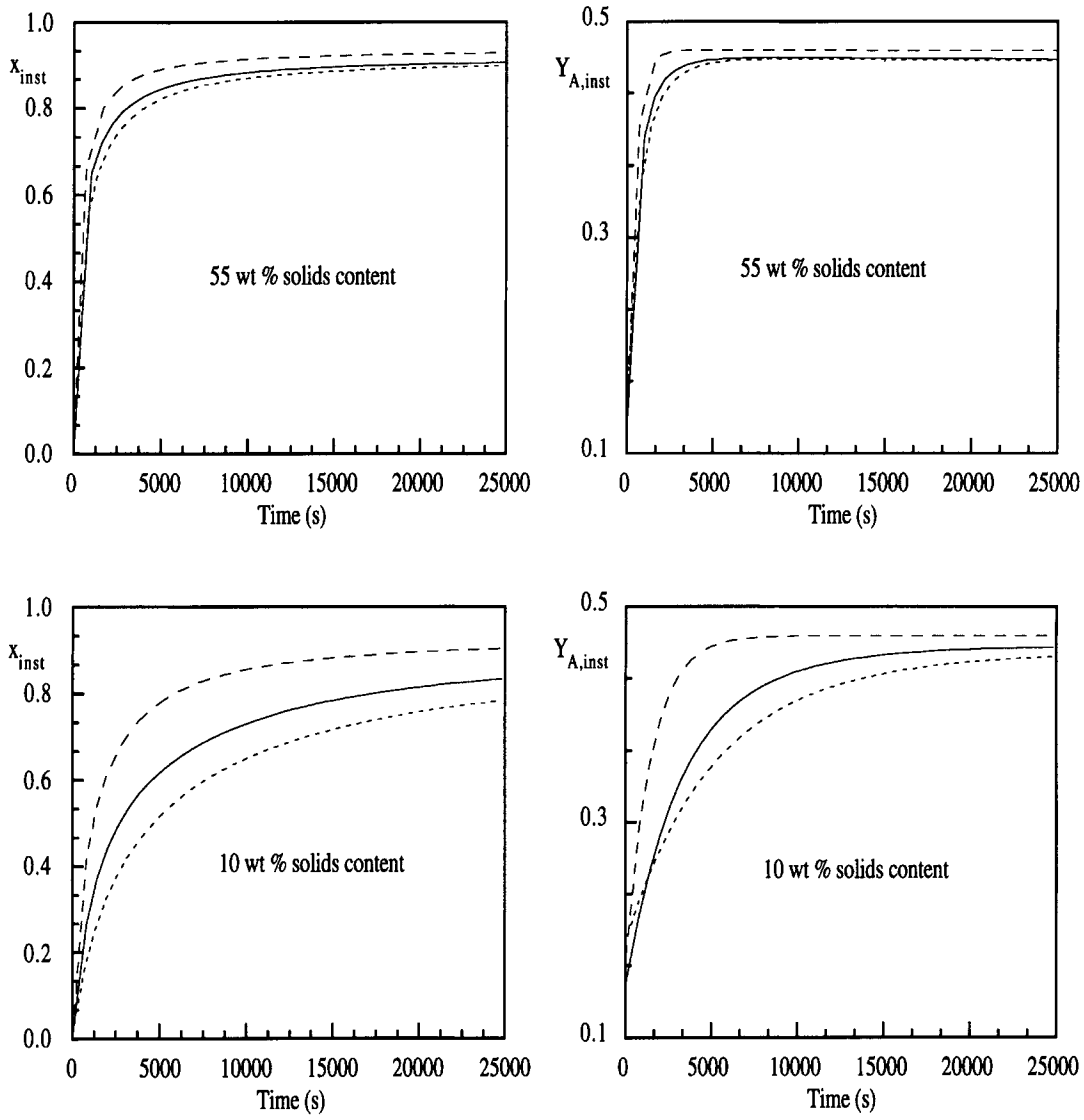

Figure 11 Effect of solids content and monomer partition model on the simulated results of the instantaneous conversion and instantaneous copolymer composition in the semicontinuous emulsion copolymerization of VAc and MA under starved conditions. (—) Morton, (• • •) Maxwell, and (- - -) constant partition coefficients.

higher solids contents. It is interesting to compare the effect of the monomer partition model on the copolymer composition for the starved and semistarved processes. Under starved conditions, the predictions of the model using constant partition coefficients were significantly different from those obtained with the Morton model. Smaller differences were found between the Maxwell and Morton models (Fig. 11). Figure 16 shows the reasons for the differences between the starved and semistarved processes. In this figure, the effect of the polymer volume fraction in the polymer particles, ϕ_p^P, on the monomer partition coefficient is presented. It can be seen that the differences in the predictions of the three models increased when ϕ_p^P increased. The starved process proceeds at high ϕ_p^P values and hence the differences between the predictions of the models were larger than for the semistarved process in which ϕ_p^P is low.

VAc/BuA Copolymerization

The results were similar to those presented for the VAc/MA emulsion copolymerization system,

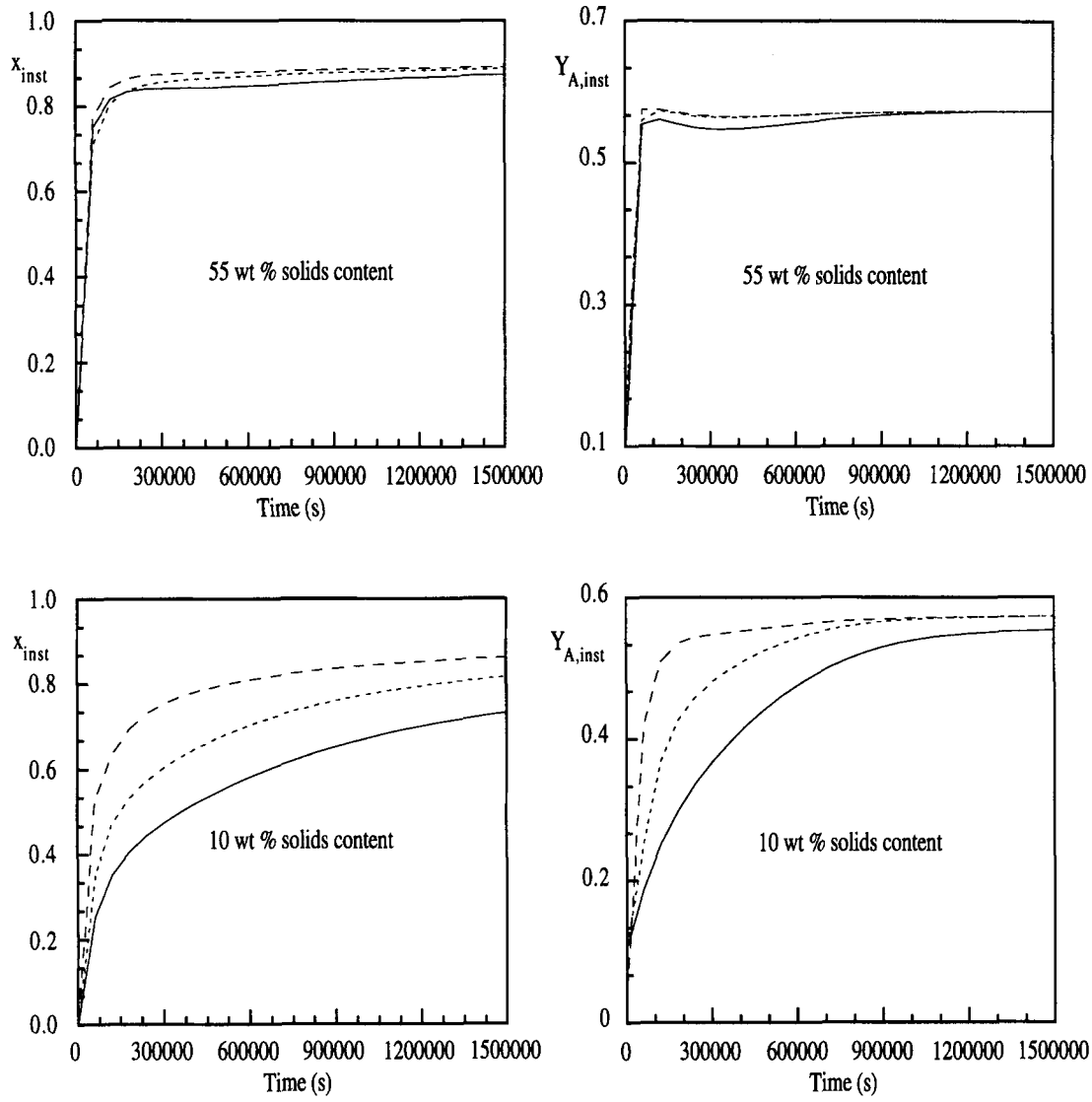

Figure 12 Effect of solids content and monomer partition model on the simulated results of the instantaneous conversion and instantaneous copolymer composition calculated for the semicontinuous emulsion copolymerization of VAc and BuA under starved conditions. (—) Morton, (• • •) Maxwell, and (- - -) constant partition coefficients.

namely, the monomer partition model had almost no effect on the instantaneous copolymer composition (Fig. 17).

St/MAA Copolymerization

Figure 18 shows that the instantaneous copolymer composition calculated with constant monomer partition coefficients deviated significantly from the desired value. Those differences increased when the solids content was decreased.

An interesting result found was that arbitrarily varying the reactivity ratios for a given system, the larger the difference in reactivity ratios, the lesser the effect of the monomer partitioning system. This result was independent of the water solubilities of the monomers.

CONCLUSIONS

In this article, a criterion for the choice of the monomer partition model in mathematical modeling of emulsion copolymerization systems was devel-

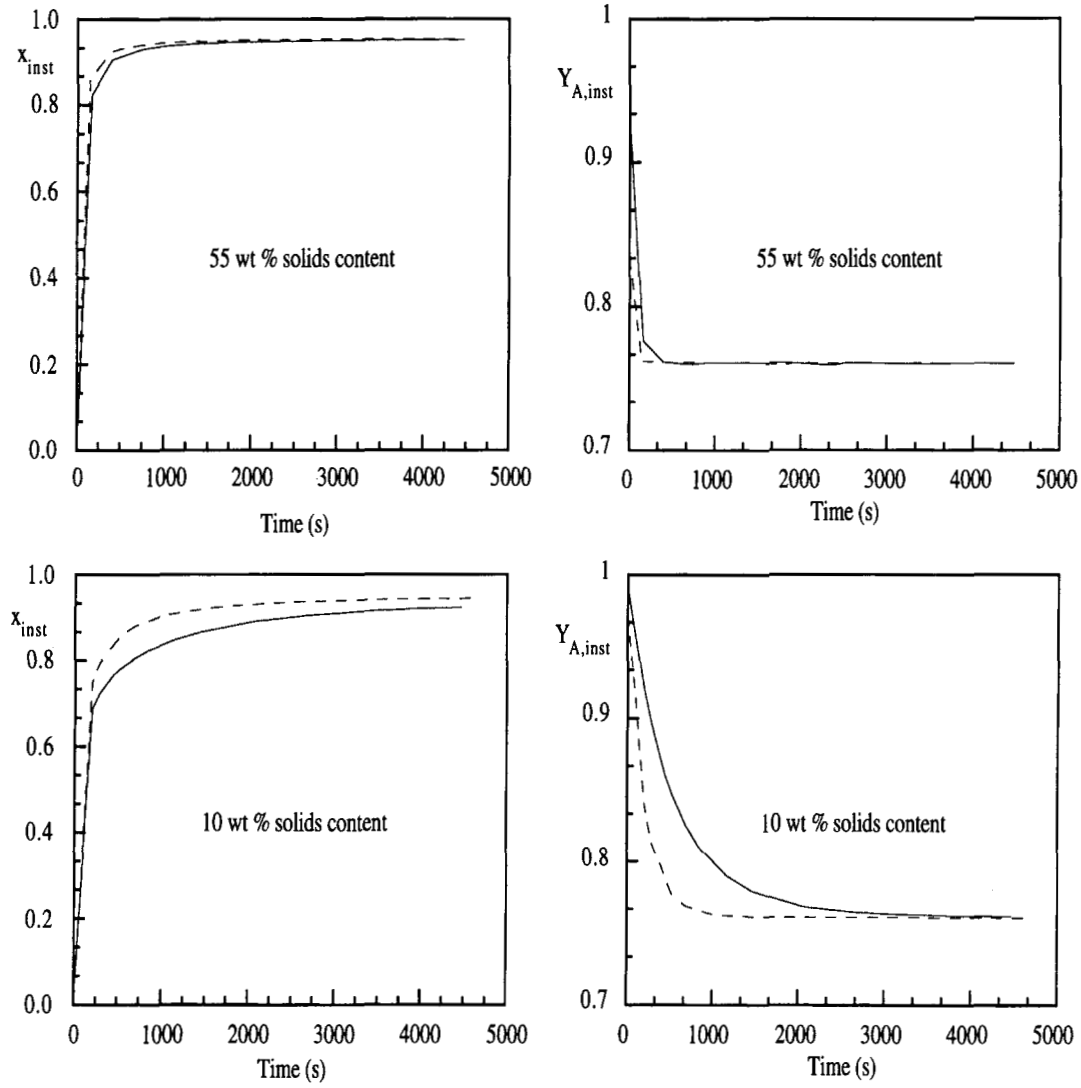

Figure 13 Effect of solids content and monomer partition model on the simulated results of the instantaneous conversion and instantaneous copolymer composition calculated for the semicontinuous emulsion copolymerization of St and MAA under starved conditions. (—) Morton and (---) constant partition coefficients.

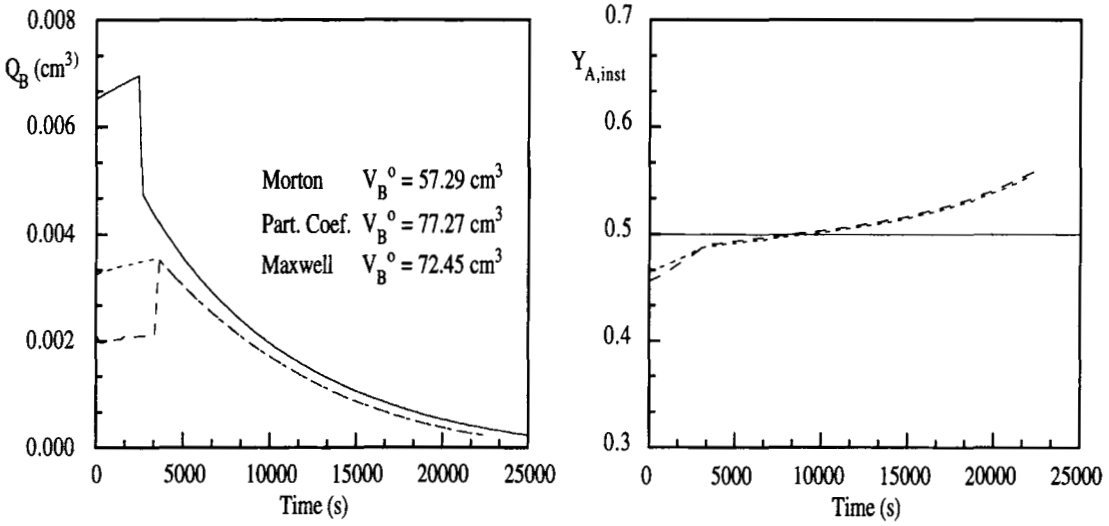

Figure 14 Volumetric feed rate profiles of St and time evolution of the copolymer composition for the 30 wt % solids content semistarved copolymerization of BuA and St. (—) Morton, (· · ·) Maxwell, and (---) constant partition coefficients.

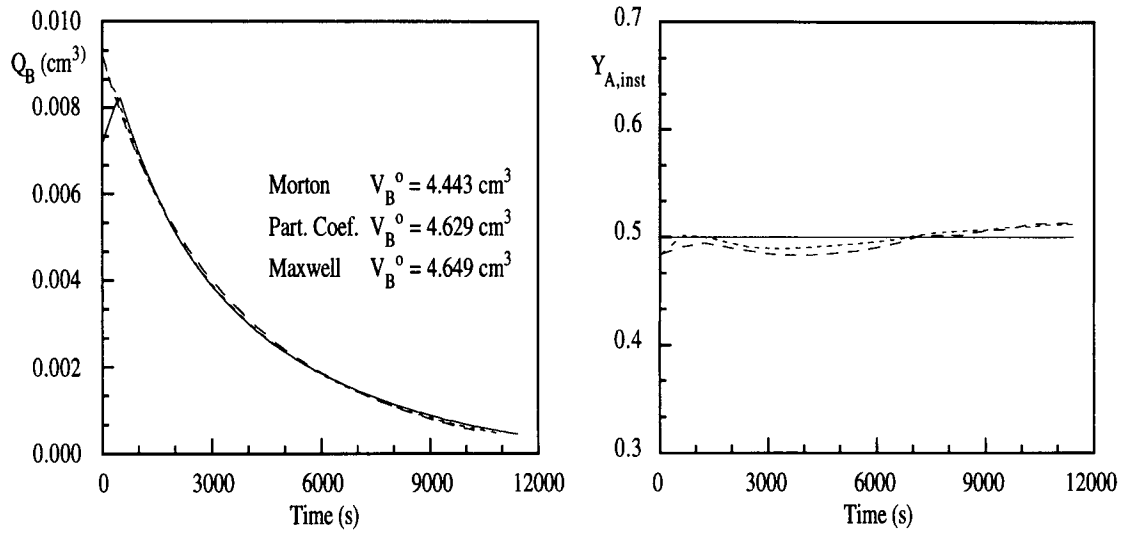

Figure 15 Volumetric feed rate profiles of MA and time evolution of the copolymer composition for the 30 wt % solids content semistarved copolymerization of VAc and MA. (—) Morton, (· · ·) Maxwell, and (---) constant partition coefficients.

oped. Seeded emulsion copolymerizations of four monomer systems with a wide variety of reactivity ratios and water solubilities were simulated using monomer partition models of different complexity. The simulations included different processes (batch, semicontinuous under starved conditions, and semicontinuous optimal semistarved), solids contents, and amounts of seed. These simulations allowed the recommendations presented in Table V to be elaborated. The recommendations were made on the basis of choosing the simplest but sufficiently accurate model.

Batch Emulsion Copolymerizations

The Morton model must be used in the case of low solids content polymerizations, unseeded medium solids content systems, or when completely water soluble monomers are included in the reaction recipe. Constant partition coefficients are adequate for

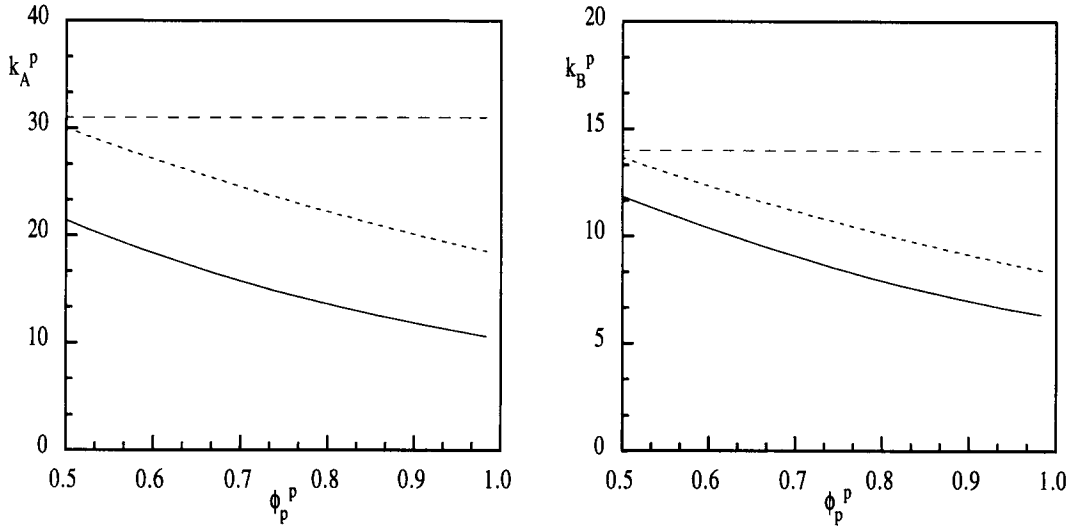

Figure 16 Partition coefficients calculated by the three models for the VAc/MA system. (—) Morton, (· · ·) Maxwell, and (---) constant partition coefficients.

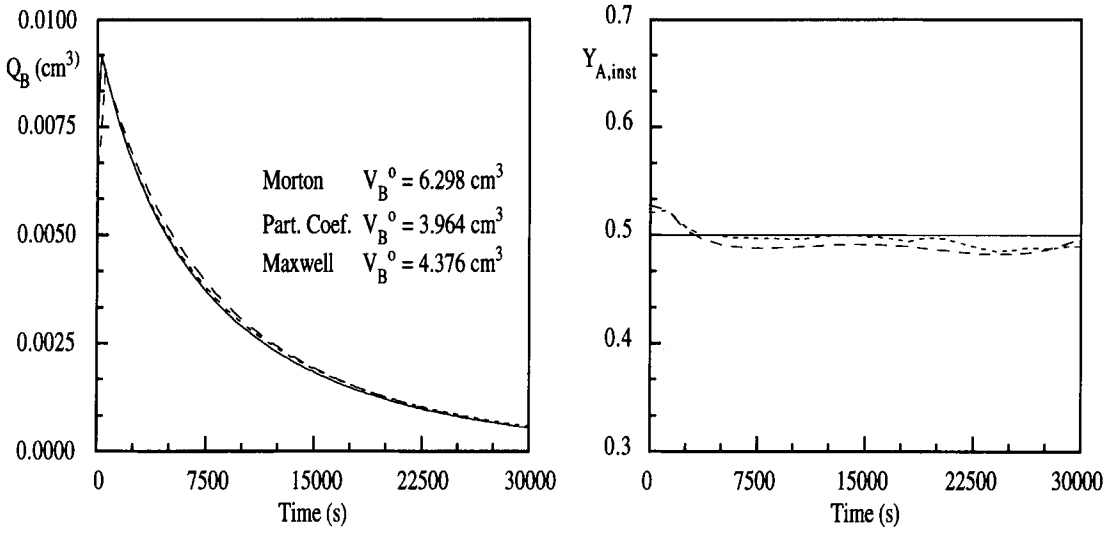

Figure 17 Volumetric feed rate profiles of BuA and cut the time evolution of the copolymer composition for the 30 wt % solids content semistarved copolymerization of VAc and BuA. (—) Morton, (· · ·) Maxwell, and (- - -) constant partition coefficients.

medium solids content seeded polymerizations and high solids content seeded and unseeded systems.

Semicontinuous Emulsion Copolymerizations Under Starved Conditions

The Morton model is recommended for low solids content recipes. The Maxwell model gives good results for medium solids contents, and this model or the model of constant partition coefficients can be used for high solids content polymerizations.

Semicontinuous Optimal Semistarved Emulsion Copolymerizations

The Morton model must be used when completely water soluble monomers are included in the poly-

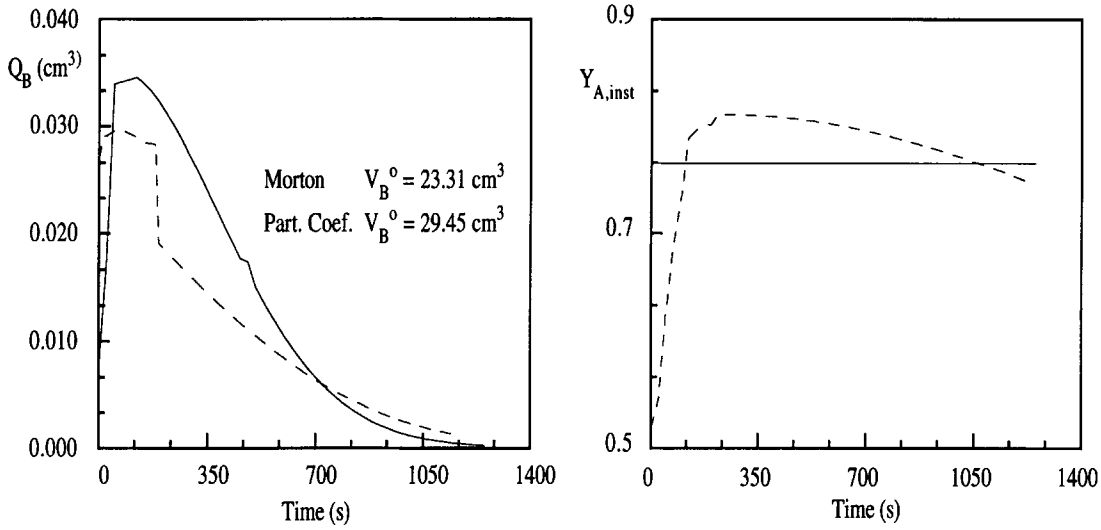

Figure 18 Volumetric feed rate profiles of MAA and time evolution of the copolymer composition for the 30 wt % solids content semistarved copolymerization of St and MAA. (—) Morton and (- - -) constant partition coefficients.

Table V Summary of Monomer Partition Models Recommended

Process	Monomer Water Solubility	Solids Content (%)	Seed/Monomer Ratio	Recommended Monomer Partition Model
Batch	Total	—	—	Morton
	Partial	10	—	Morton
		30	< 0.10	Morton
		30	> 0.10	Constant partition coefficients
		55	> 0.03	Constant partition coefficients
Starved	—	10	—	Morton
	Total	30–45	—	Morton
	Partial	30–45	—	Maxwell
	—	55	—	Constant partition coefficients
Semistarved	Total	—	—	Morton
	Partial	> 30	—	Constant partition coefficients

merization recipe. For partially water-soluble monomers, the model of constant partition coefficients provides good enough results.

The financial support by the CICYT (Grant MAT 91-01950) is greatly appreciated. Luis Gugliotta acknowledges the scholarship from the CONICET (Consejo Nacional de Investigaciones Científicas y Técnicas, República Argentina) and the grant from the Diputación Foral de Gipuzkoa.

NOMENCLATURE

A, B Monomers A and B, respectively (mol).
A^0, B^0 Monomers A and B initially charged into the reactor (mol).
d_p^0 Initial unswollen polymer particle diameter (nm).
D_p Diffusion coefficient of the single-unit radicals in the monomer swollen polymer particles (cm^2/s).
D_w Diffusion coefficient of the radicals in the aqueous phase (cm^2/s).
f Efficiency factor for initiator decomposition.
F Radical capture efficiency.
ΔG_i^j Molar free energy of monomer i in the phase j (J/mol).
$[i]_j$ Monomer concentration of monomer i in the phase j (mol/cm^3).
I^0 Moles of initiator initially charged into the reactor (mol).
k_{fij} Monomer chain transfer constant (cm^3/mol s).
k_I Rate constant of initiator decomposition (s^{-1}).
k_i^j Partition coefficient of monomer i between the phase j and aqueous phase.
k_{pij} Propagation rate constant (cm^3/mol s).
k_{tij} Termination rate constant (cm^3/mol s).
m_{ik} Ratio of the equivalent number of segments of the components i and k.
N_A Avogadro's number.
N_p Total number of polymer particles.
Q_B Volumetric feed rate of monomer B (cm^3/s).
r_A, r_B Reactivity ratios.
r_j Radius of phase j (cm).
R Gas constant [J/(mol K)].
R_{pi} Polymerization rate of monomer i (mol/s).
T Absolute temperature (K).
v_i Molar volume of monomer i (cm^3/mol).
V_i Total volume of free monomer i (cm^3).
V^j Total volume of phase j (cm^3).
V_i^j Total volume of monomer i in the j phase (cm^3).
V_{pol} Total volume of polymer in the latex (cm^3).
W Total volume of water (cm^3).
x Overall molar conversion.
x_i Instantaneous conversion of monomer i.
Y_A Cumulative molar copolymer composition (moles of monomer A in the copolymer/moles of monomers A and B in the copolymer).
$Y_{A,inst}$ Instantaneous molar copolymer composition [moles of monomer A instantaneously incorporated to the copolymer/moles of monomer A and B instantaneously incorporated to the copolymer; $R_{pA}/(R_{pA} + R_{pB})$].

Greek Symbols

ϕ_i^j Volumetric fraction of component i in the phase j.

$\phi_{i,\text{sat}}^{\text{w}}$ Volumetric fraction of component i in the aqueous phase under saturation conditions for a single monomer.

$\phi_{i,\text{sat}}^{\prime\text{w}}$ Volumetric fraction of component i in the aqueous phase under saturation conditions with two monomers.

$\phi_{i,\text{sat}}^{\text{p}}$ Volumetric fraction of the species i in the particles of homopolymer i swollen with a single monomer under saturation conditions.

$\phi_{i,\text{sat}}^{\prime\text{p}}$ Volumetric fraction of the species i in swollen particles of copolymer under saturation conditions.

σ Interfacial tension (dyne/cm).

χ_{ik} Interaction parameter between species i and k.

χ_{ipj} Interaction parameter of monomer i with homopolymer j.

APPENDIX I: MODELS FOR ESTIMATION OF MONOMER CONCENTRATIONS IN DIFFERENT PHASES

For the prediction of the monomer concentrations in the different phases the overall material balances for the monomers have to be solved together with the equilibrium equations.

Assuming that both the volume change by mixing and the solubility of water in the monomer and polymer phases are negligible, the overall material balances (or volume balances) can be written as follows:

$$V_i = V_i^{\text{d}} + V_i^{\text{w}} + V_i^{\text{p}} \quad i = \text{A, B} \tag{A.1}$$

$$V^{\text{w}} = W + V_{\text{A}}^{\text{w}} + V_{\text{B}}^{\text{w}} \tag{A.2}$$

$$V^{\text{p}} = V_{\text{A}}^{\text{p}} + V_{\text{B}}^{\text{p}} + V_{\text{pol}} \tag{A.3}$$

$$V^{\text{d}} = V_{\text{A}}^{\text{d}} + V_{\text{B}}^{\text{d}} \tag{A.4}$$

where V_i is the total volume of monomer i; V_i^{d}, V_i^{w} and V_i^{p} are the total volumes of monomer i in monomer droplets, aqueous phase, and polymer particles, respectively; V^{w}, V^{p}, and V^{d} represent the total volumes of aqueous phase, polymer particles, and monomer droplets, respectively; W is the total volume of water; and V_{pol} the total volume of polymer.

The equilibrium equations depend on the model used. The following three models were used in the present work.

Morton Extension of Flory–Huggins Theory[1–3]

The thermodynamic equilibrium is reached when the partial molar free energy of each monomer is equal in each of the three phases. Under these conditions, the following relationships can be written:

Aqueous phase (w) – monomer droplets (d)

$$\left(\frac{\Delta G}{RT}\right)_i^{\text{w}} = \left(\frac{\Delta G}{RT}\right)_i^{d} \quad i = \text{A, B.} \tag{A.5}$$

Polymer particles (p) – aqueous phase (w)

$$\left(\frac{\Delta G}{RT}\right)_i^{\text{p}} = \left(\frac{\Delta G}{RT}\right)_i^{\text{w}} \quad i = \text{A, B} \tag{A.6}$$

where the partial molar free energy of each monomer in the different phases can be calculated as follows.[3]

$$\left(\frac{\Delta G}{RT}\right)_i^{j} = \ln \phi_i^j + \sum_{k=1}^{n} (1 - m_{ik})\phi_k^j + \sum_{k=1\neq i}^{n} \chi_{ik}(\phi_k^j)^2 + \sum_{k=1\neq i}^{n-1} \sum_{l=k+1\neq i}^{n} \phi_k^j \phi_l^j (\chi_{ik} + \chi_{il} - \chi_{kl} m_{ik}) + \frac{2\sigma v_i}{r_j RT}$$

$$i = \text{A, B} \quad \text{and} \quad j = \text{d, p, w} \tag{A.7}$$

where ϕ_i^j is the volume fraction of monomer i in phase j, m_{ik} the ratio of the equivalent number of segments of components i and k; v_i the molar volume of monomer i; r_j the radius of phase j; σ the interfacial tension; R the universal gas constant; T the absolute temperature; and χ_{ik} the interaction parameter. The interaction parameter of monomer i with the copolymer is calculated as follows:

$$\chi_{ip} = Y_{\text{A}}\chi_{ip\text{A}} + (1 - Y_{\text{A}})\chi_{ip\text{B}} \tag{A.8}$$

where χ_{ipj} is the interaction parameter of monomer i with homopolymer j and Y_{A} the cumulative molar composition of A in the copolymer.

Maxwell et al.[4–7] Semiempirical Equations

Intervals I and II ($V^d > 0$)

For the case in which there are droplets in the system, Maxwell proposed the following relationship, here expressed in terms of volumes, to describe the equilibrium between phases of partially water soluble monomers:

Aqueous phase (w) – monomer droplets (d)

$$V_i^{\text{w}} = \frac{V^{\text{w}}}{V^{\text{d}}} V_i^{\text{d}} \phi_{i,\text{sat}}^{\text{w}} \quad i = \text{A, B.} \tag{A.9}$$

Polymer particles (p) – monomer droplets (d)

$$V_A^p = V_A^d \frac{V^p}{V^d}\left\{(\phi_{A,sat}^p - \phi_{B,sat}^p)\frac{V_A^d}{V^d} + \phi_{B,sat}^p\right\} \quad (A.10)$$

$$V_B^p = V_B^d \frac{V^p}{V^d}\left\{(\phi_{B,sat}^p - \phi_{A,sat}^p)\frac{V_B^d}{V^d} + \phi^p{}_{A,sat}\right\} \quad (A.11)$$

where $\phi_{i,sat}^w$ is the volumetric fraction of monomer i (i = A, B) in the aqueous phase under homosaturation conditions and $\phi_{A,sat}^p$ and $\phi_{B,sat}^p$ the volumetric fractions of monomers A and B in particles of homopolymers A and B under homosaturation conditions, respectively. Here, homosaturation refers to the saturation when the polymer particles are swollen with a single monomer.

Interval III ($V^d = 0$)

In the absence of monomer droplets, the equations proposed by Maxwell et al.[4-7,10,11] can be written as follows:

$$V_A^w = \phi_{A,sat}'^w V^w\left[\frac{V_A^p}{V^p \phi_{A,sat}'^p}\exp\left(\frac{V_{pol}}{V^p} - \phi_{p,sat}'^p\right)\right] \quad (A.12)$$

$$V_B^w = \phi_{B,sat}'^w V^w\left[\frac{V_B^p}{V^p \phi_{B,sat}^p}\exp\left(\frac{V_{pol}}{V^p} - \phi_{p,sat}'^p\right)\right] \quad (A.13)$$

where $\phi_{A,sat}'^p$, $\phi_{B,sat}'^p$, and $\phi_{p,sat}'^p$ are volumetric fractions of A, B, and polymer in the copolymer particles under saturation conditions, respectively; and $\phi_{A,sat}'^w$ and $\phi_{B,sat}'^w$ the volumetric fractions of monomers A and B in water under saturation conditions. In both cases the swelling is carried out with a mixture of two monomers.

Constant Partition Coefficients

In this case, the equilibrium is described through partition coefficients that are considered constant throughout the reaction and defined by:

$$k_i^j = \frac{\phi_i^j}{\phi_i^w} \quad i = A, B \quad \text{and} \quad j = p, d \quad (A.14)$$

$$\phi_i^j = \frac{V_i^j}{V^j} \quad (A.15)$$

APPENDIX II: ALGORITHM TO CALCULATE MONOMER DISTRIBUTION BETWEEN PHASES USING MAXWELL SEMIEMPIRICAL EQUATIONS

The models described in Appendix I consist of a set of nonlinear algebraic equations. They can be solved by means of a general purpose algorithm such as the Newton–Raphson method. However, the use of specific algorithms provides substantial computer time savings. Therefore, in this work, the method proposed by Armitage et al.[32] was used when the equilibrium was described by the Morton model and a variation of the method due to Omi[33] was used when the constant partition coefficients model was utilized. In the following a method is proposed to describe the equilibrium between the phases when the Maxwell equations are used.

Intervals I and II ($V_d > 0$)

Equations (A.1–A.4) and (A.9–A.11) of Appendix I are a set of nine equations with nine unknowns V_A^p, V_B^p, V_A^d, V_B^d, V_A^w, V_B^w, V^w, V^p, and V^d). Substituting Eqs. (A.9) and (A.10) into Eq. (A.1) for i = A, the following expression can be obtained:

$$V_A^d = -\frac{b}{2} \pm \frac{1}{2}(b^2 + 4c)^{1/2} \quad (A.16)$$

with

$$b = \frac{V^{d^2}\left(1 + \phi_{B,sat}^p \frac{V^p}{V^d} + \phi_{A,sat}^w \frac{V^w}{V^d}\right)}{V^p(\phi_{A,sat}^p - \phi_{B,sat}^p)} \quad (A.17)$$

$$c = \frac{V_A V^{d^2}}{V^p(\phi_{A,sat}^p - \phi_{B,sat}^p)}. \quad (A.18)$$

Similarly, substitution of Eqs. (A.9) and (A.11) in (A.1) for i = B, gives:

$$V_B^d = -\frac{d}{2} \pm \frac{1}{2}(d^2 + 4e)^{1/2} \quad (A.19)$$

with

$$d = \frac{V^{d^2}\left(1 + \phi_{A,sat}^p \frac{V^p}{V^d} + \phi_{B,sat}^w \frac{V^w}{V^d}\right)}{V^p(\phi_{B,sat}^p - \phi_{A,sat}^p)} \quad (A.20)$$

$$e = \frac{V_B V^{d^2}}{V^p(\phi_{B,sat}^p - \phi_{A,sat}^p)}. \quad (A.21)$$

Note that the positive root must be utilized in Eq. (A.16) and the negative one in Eq. (A.19) if $\phi_{A,sat}^p > \phi_{B,sat}^p$; and conversely if $\phi_{A,sat}^p < \phi_{B,sat}^p$. On the other hand, when $\phi_{A,sat}^p = \phi_{B,sat}^p$, Eqs. (A.10) and (A.11) must be replaced by:

$$V_A^p = V_A^d \frac{V^p}{V^d} \phi_{B,sat}^p \quad (A.22)$$

$$V_B^p = V_B^d \frac{V^p}{V^d} \phi_{A,sat}^p. \quad (A.23)$$

Combination of Eqs. (A.22), (A.23), and (A.1) gives:

$$V_A^d = \frac{V_A}{1 + \frac{V^p}{V^d} \phi_{B,sat}^p + \frac{V^w}{V^d} \phi_{A,sat}^w} \quad (A.24)$$

$$V_B^d = \frac{V_B}{1 + \frac{V^p}{V^d} \phi_{A,sat}^p + \frac{V^w}{V^d} \phi_{B,sat}^w}. \quad (A.25)$$

Equations (A.24) and (A.25) should be used instead of Eqs. (A.16) and (A.19) when $\phi_{A,sat}^p = \phi_{B,sat}^p$.

The following algorithm, based on previous equations, is proposed in order to calculate monomer volumes in each phase:

1. Guess initial values of V^d, V^p, and V^w.
2. Calculate V_A^d and V_B^d from Eqs. (A.16) and (A.19) [or Eqs. (A.24) and (A.25) when $\phi_{A,sat}^p = \phi_{B,sat}^p$].
3. Calculate V_A^p and V_B^p using Eqs. (10–11)) [or Eqs. (A.22) and (A.23) when $\phi_{A,sat}^p = \phi_{B,sat}^p$].
4. Calculate V_A^w and V_B^w with Eq. (A.9).
5. Calculate V^w, V^p, and V^d from Eqs. (A.2)–(A.4).
6. Repeat steps 2–5 until convergence in V^w, V^p, and V^d is reached.

Interval III ($V^d = 0$)

Equations (A.1)–(A.3) with $V_i^d = 0$ and eqs. (A.12) and (A.13) of Appendix I are a set of six equations with six unknowns (V_A^p, V_B^p, V_A^w, V_B^w, V^p, and V^w). Substituting Eq. (A.12) into Eq. (A.1) with i = A and rearranging, the following equation results:

$$V_A^p = \frac{V_A}{1 + \frac{\phi'^w_{A,sat} V^w}{\phi'^p_{A,sat} V^p} \exp\left(\frac{V_{pol}}{V^p} - \phi'^p_{p,sat}\right)}. \quad (A.26)$$

Similarly for V_B^p

$$V_B^p = \frac{V_B}{1 + \frac{\phi'^w_{B,sat} V^w}{\phi'^p_{B,sat} V^p} \exp\left(\frac{V_{pol}}{V^p} - \phi'^p_{p,sat}\right)}. \quad (A.27)$$

The following algorithm of direct substitution was used to calculate the monomer volumes in the two phases:

1. Guess initial values of V^p and V^w.
2. Calculate V_A^p and V_B^p from Eqs. (A.26) and (A.27).
3. Calculate V_A^w and V_B^w using Eqs. (A.12) and (A.13).
4. Calculate V^w and V^p with Eqs. (A.2) and (A.3).
5. Repeat steps 2–4 until convergence in V^w and V^p is obtained.

Equations (A.12) and (A.13) include a correction term that is calculated from saturation concentrations in aqueous and polymeric phases. The correction term ensures the continuity in the evolution of monomer concentrations. In practice, when monomer droplets are present at the beginning of reaction, good results are obtained choosing $\phi'^p_{i,sat} = \phi_i^p$; $v^d = 0$ and $\phi'^w_{i,sat} = \phi_i^w$; $v^d = 0$. On the other hand, when monomer droplets are absent at the beginning of polymerization, experimental information of $\phi'^p_{i,sat}$ and $\phi^w{}_{i,sat}$ is required, or should be estimated from homosaturation volumetric fractions.[6]

REFERENCES

1. M. Morton, S. Kaizerman, and M. W. Altier, *J. Colloid Sci.*, **9**, 300 (1954).
2. J. Guillot, *Acta Polym.*, **32**, 593 (1981).
3. J. Ugelstad, P. C. Mork, H. R. Mfutakamba, et al., in *Science and Technology of Polymer Colloids*, Vol. 1, G. W. Poehlein, R. H. Ottewill, and J. W. Goodwin, Eds., NATO ASI Ser., Ser. E, 1983.
4. I. A. Maxwell, J. Kurja, G. H. J. Van Doremaele, and A. L. German, *Makromol. Chem.*, **193**, 2049 (1992).
5. I. A. Maxwell, J. Kurja, G. H. J. Van Doremaele, and A. L. German, *Makromol. Chem.*, **193**, 2065 (1992).
6. L. F. J. Noël, I. A. Maxwell, and A. L. German, *Macromolecules*, **26**, 2911–2918 (1993).
7. I. A. Maxwell, L. F. J. Noël, H. A. S. Schoonbrood, and A. L. German, *Makromol. Chem. Theory Simul.*, **2**, 269–274 (1993).
8. P. J. Flory, *Principles of Polymer Science*, Cornell University Press, Ithaca, New York, 1953; *J. Chem. Phys.*, **10**, 51 (1942).
9. M. L. Hüggins, *J. Phys. Chem.*, **46**, 151 (1942); *J. Am. Chem. Soc.*, **64**, 1712 (1942).
10. J. Guillot, *Makromol. Chem. Suppl.*, **10**, 235 (1985).
11. J. Delgado, Ph.D. dissertation, Lehigh University, 1986.
12. R. N. Mead and G. W. Poehlein, *Ind. Eng. Chem. Res.*, **27**, 2283 (1988).

13. G. Arzamendi and J. M. Asua, *J. Appl. Polym. Sci.*, **38,** 2019 (1989).
14. J. Dimitratos, C. Georgakis, M. S. El-Aasser, and A. Klein, *Comp. Chem. Eng.*, **13,** 21 (1989).
15. G. L. Shoaf, Ph.D. dissertation, Georgia Institute of Technology, 1989.
16. D. J. Kozub, Ph.D. dissertation, McMaster University, Hamilton, Ontario, Canada, 1989.
17. G. Arzamendi and J. M. Asua, *Makromol. Chem., Macromol. Symp.*, **35/36,** 249 (1990).
18. G. L. Shoaf and G. W. Poehlein, *Ind. Eng. Chem. Res.*, **29,** 1701 (1990).
19. B. Urquiola, G. Arzamendi, J. R. Leiza, et al., *J. Polym. Sci. A*, **29,** 169 (1991).
20. D. M. Lange and G. W. Poehlein, *Polym. Reaction Eng.*, **1,** 41 (1992–1993).
21. D. H. Napper and A. G. Parts, *J. Polym. Sci.*, **61,** 113 (1962).
22. M. J. Ballard, D. H. Napper, and R. G. Gilbert, *J. Polym. Sci., Polym. Chem. Ed.*, **22,** 3225 (1984).
23. I. A. Maxwell, B. R. Morrison, R. G. Gilbert, and D. H. Napper, *Macromolecules*, **24,** 1629 (1991).
24. J. R. Leiza, J. C. de la Cal, G. R. Meira, and J. M. Asua, *Polym. Reaction Eng.*, **1,** 46 (1992–1993).
25. A. Urretabizkaia, J. R. Leiza, and J. M. Asua, *AIChE*, to appear.
26. J. Guillot and L. Rios-Guerrero, *Makromol. Chem.*, **183,** 1979 (1982).
27. W. Ramirez-Marquez, and J. Guillot, *Makromol. Chem.*, **189,** 361 (1988).
28. W. Ramirez-Marquez, and J. Guillot, *Makromol. Chem.*, **189,** 379 (1988).
29. G. Arzamendi, J. R. Leiza, and J. M. Asua, *J. Polym. Sci. A*, **29,** 1549 (1991).
30. G. Arzamendi and J. M. Asua, *Ind. Eng. Chem. Res.*, **30,** 1342 (1991).
31. R. G. Gilbert and D. H. Napper, *JMS-Rev. Macromol. Chem. Phys.*, **C23,** 127 (1983).
32. P. Armitage, J. C. de la Cal, and J. M. Asua, *J. Appl. Polym. Sci.*, to appear.
33. S. Omi, *Zayro Gijutsu*, **4,** 29 (1986).
34. J. L. Gardon, *J. Polym. Sci. A-1*, **6,** 643 (1968).
35. F. C. Leonard, *Vinyl and Diene Monomers*, Parts I–III, J. Wiley, New York, 1970–1971.
36. A. Echevarria, G. R. Meira, J. C. de la Cal, and J. M. Asua, *Chem. Eng. Sci.*, to appear.
37. J. Brandrup and H. Immergut, Eds., *Polymer Handbook*, 3rd ed., Wiley Interscience, New York, 1989.
38. A. Cruz Rivera, L. Rios-Guerrero, C. Monnet, B. Schlund, J. Guillot, and C. Pichot, *Polymer*, **60,** 1873 (1989).

Received February 15, 1994
Accepted July 31, 1994